Effects of Nanomaterials on the Electro-Osmotic Consolidation of Soft Soils

Gang Li[1], Jia Liu[2,*], Huanhuan Li[1], Shufeng Chen[1], Rui Zhang[1]

[1] Shaanxi Key Laboratory of Safety and Durability of Concrete Structures, Xijing University, Xi'an, Shaanxi 710123, China;
[2] School of Geological Engineering and Geomatics, Chang'an University, Xi'an, Shaanxi 710054, China.
*E-mail: 15929935077@163.com

Soft soil is characterized by a high water content (w), high void ratio, high compressibility, poor permeability, and low shear strength (S); therefore, it is not suitable as a natural foundation without proper treatment. In this study, axisymmetric electro-osmotic (EO) consolidation of soft soil was carried out, and the change laws of current (I), potential (U), w, water discharge (V), pH, S, and bearing capacity (B) during the EO process were analyzed. The consolidation effect was enhanced by the addition of SiO_2 nanoparticles or Fe_3O_4 nanosolution, and the mechanism of EO consolidation was determined by analyzing the macroscopic properties and microstructure of the soil. The results showed that the I and U in soil decreased with time (t), while the V increased with t. Near the anode, the w and pH were low, but the S and B were high. The soil cracks were centered on the cathode and spread out in a cross pattern that extended to the anode. In addition, ion exchange occurred on the surface of the soil particles and inside the crystal layer, which produced a thinner electrical double layer, lower zeta potential, and lower water absorption capacity of the particles. To improve the consolidation effects, the best concentrations of nano-SiO_2 and nano-Fe_3O_4 were 3‰ and 2‰, respectively.

1. INTRODUCTION

Soft soil is widely distributed in coastal areas and has a high water content (w), high void ratio, high compressibility, poor permeability, and low shear strength (S). As a result, soft soil is not suitable as a natural foundation without proper treatment [1-2]. An effective method for treating soft clay foundations is drainage consolidation, which includes vacuum preloading, surcharge preloading, dewatering preloading, and electro-osmotic (EO) methods. However, vacuum preloading and dewatering preloading methods have high construction requirements at the treatment boundary. The drainage consolidation rate is affected by the hydraulic conductivity of the clay, and the expected

consolidation effect is not easily achieved. The surcharge preloading method is limited by the source of the surcharge materials and may cause foundation instability, so this method is not suitable for shorter construction projects. The EO method can effectively and quickly improve the bearing capacity (B) of the foundation and will not cause foundation instability, so it has excellent application prospects. Sun et al. [3] indicated that the drainage time (t) of EO with electric vertical drains (EVDs) was longer than that with metal electrodes, which is beneficial to increasing the strength. Zhou et al. [4] conducted in situ EO tests on sludge foundation with electrically conductive wick drain (ECWD) and automated power supply (APS) and determined that the w of sludge decreased from 62% to 39%, whereas B increased from 0 to 74 kPa. Hu et al. [5] noted that the w of kaolin near the anode was lower than that near the cathode for a high initial pH, and sodium addition increased the drainage rate and water discharge (V). Martin et al. [6-7] noted that the improvement of EO contains polarity reversal, intermittent current (I), chemical solution and geo-synthetics, and the zeta potential is proportional to the permeability of EO. Xue et al. [8] pointed out that the potential (U) loss was attributed to anode corrosion, and high voltage and temperature were beneficial to reducing w and increasing S. Liu et al. [9] noted that $CaCl_2$ solution can improve the EO consolidation than KCl and NaCl, whereas excessive salt solutions will reduce the consolidation efficiency. Fu et al. [10] indicated that the polarity reversal method can improve the drainage effect while increasing the energy consumption. For an actual project, the method of reduced reverse electrifying period was better than the intermittent I method. Based on the EO tests, Teng et al. [11] demonstrated that the U distributions were different between an actual test and traditional consolidation theory due to applied U losses; therefore, a correction model for U distribution was established. Zhang et al. [12] compared the effects of iron, copper, aluminum, and novel composite electrode materials on the EO consolidation of silt soft soil. They discovered that the novel electrode material significantly improved the soil strength, because 75% (by area) of the soil achieved a strength of 160 kPa after consolidation, and the corrosion on the novel composite electrode was significantly lower than that on the metal electrode. Xie et al. [13] pointed out that corrosion had a minimal effect on the electrode-soil contact resistance and no significant impact on drainage during the entire EO process. Increasing the conductive area ratio reduced the contact resistance and increased the I, and the optimal conductive area ratio of the anode was 0.47. Zang et al. [14] concluded that the factors that influence the EO drainage of organism-contaminated soil followed the order $U>t>w>CaCl_2$ addition>electrode materials; the higher is the U, the more significant is the consolidation effect. Jiao et al. [15] determined that under the same w and U, intermittent I led to greater power utilization and more uniform soil after EO consolidation. In addition, the electrode corrosion caused by EO was less with low U and intermittent I.

The EO method is characterized by a short construction period and convenient equipment installation, is suitable for drainage consolidation of soft soil and its application has gradually become more popular. Researchers that have explored the EO method focus on the control factors, electrode materials, and combination methods. However, few studies address improving EO consolidation with nanomaterials. In this study, axisymmetric EO consolidation was carried out, and the consolidation effect was promoted by SiO_2 nanoparticles and Fe_3O_4 nanosolution. The effects of nanomaterials in the EO process on I, U, w, V, pH, S, and B were analyzed, and the suitability of the nanomaterials and the

optimal concentration were determined. This study provides a guideline for the application of the EO method in actual engineering.

2. EXPERIMENTAL

2.1 Materials

Silt soil that was collected from Huai'an in Jiangsu Province, China, was employed in this study. Table 1 shows the material properties of the soil sample. To reduce the error and ensure a consistent w, the undisturbed soil was dried and crushed, and an appropriate amount of water was added and evenly mixed with the crushed soil using a blender to prepare remolded soil with a w of 70%.

Table 1. Main physical parameters of soft soil

| Water content/%	Liquid limit/%	Plastic limit/%	Plasticity index	Density/(g/cm^3)
6.75	43.6	21.7	21.9	1.82

Nano-SiO$_2$ particles were purchased from Nanjing Paukert Advanced Material Co., Ltd. The particles had a size of 20 nm, a purity greater than 99.8%, a specific surface area of 280 m^2/g, and a pH value that ranges from 5 to 7. With stable chemical properties and many micropores, nano-SiO$_2$ particles feature a strong absorbent ability as well as great dispersion, suspension, and thixotropy. Appearing as a white, fluffy powder, nano-SiO$_2$ is nontoxic, tasteless, and pollution-free.

The nano-Fe$_3$O$_4$ solution utilized in this study was purchased from Hangzhou Zhitai Purification Technology Co., Ltd. Nano-Fe$_3$O$_4$ powder is magnetic and can move directionally in an external magnetic field. Nano-Fe$_3$O$_4$ powder with a specific particle size is super paramagnetic and can generate heat while retaining its chemical properties under the action of an external alternating electromagnetic field. The nano-Fe$_3$O$_4$ solution employed in this study possessed a particle size of 20-30 nm, a purity greater than 99.9%, and a particle content higher than 20%.

2.2 Modeling

The experiment was carried out in a cylindrical Plexiglass box. The box had a diameter of 400 mm, a height of 280 mm, and a wall thickness of 10 mm. Four circular slots with an inner diameter of 10 mm were set on two mutually perpendicular diameters of the bottom plate. The slots were 10 mm from the inner wall of the model. All the slots were concave downward over a distance of 5 mm to fix the anode tube. A circular slot with a diameter of 22 mm was arranged at the center of the bottom plate, which was concave downward over a distance of 5 mm to fix the cathode tube, and a drain hole with a diameter of 10 mm was set inside the slot at the center. The upper part of the model box was equipped with a 2-mm-thick circular cover with a diameter of 420 mm. Figure 1 shows a schematic of the model test. The electrode material in this study was iron. The anode was a hollow iron pipe with a

diameter of 8 mm, a wall thickness of 1 mm, and a height of 240 mm. The side of the anode tube, which was located 5 mm below the top of the tube, was drilled to make a pair of 5-mm-diameter holes to connect the wire. The cathode tube was assumed to be uniformly punched for drainage, which was a difficult process. Therefore, a Plexiglass tube (diameter of 18 mm, wall thickness of 1 mm, and height of 290 mm) was evenly wrapped with a 0.7-mm-diameter iron wire that served as the cathode, on which small holes with a diameter of 4 mm were uniformly distributed. In addition, the cathode was wrapped with a 1-mm-thick geotextile to prevent blockage of the drainage holes.
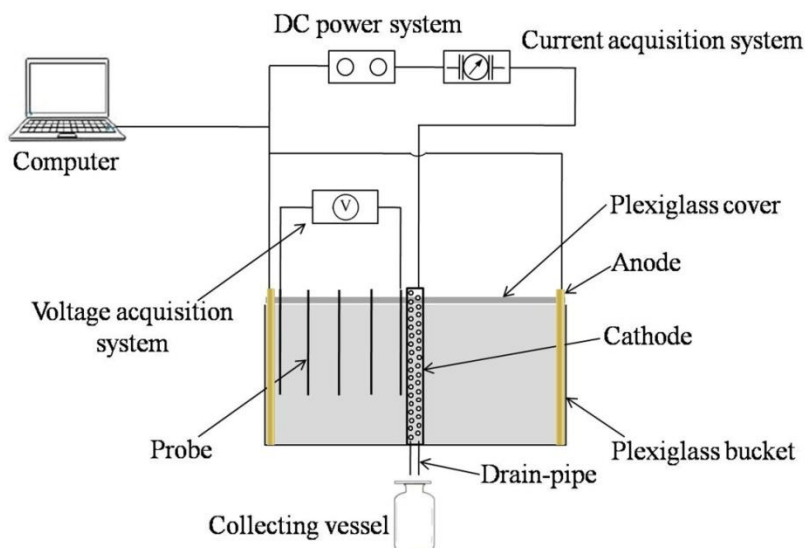
Figure 1. Schematic of the model test

2.3 Methods

As shown in Table 2, seven groups of experiments were carried out, and parallel experiments were simultaneously conducted. The experimental voltage was 30 V, and the initial *w* of the sample was set to 70.0%.

Table 2. Test scheme

Test No.	Time/h	Potential/V	Nanomaterials	Concentration/‰
T1	72	30	--	--
T2	72	30	nano-SiO_2	1
T3	72	30	nano-SiO_2	2
T4	72	30	nano-SiO_2	3
T5	72	30	nano-Fe_3O_4	1
T6	72	30	nano-Fe_3O_4	2
T7	72	30	nano-Fe_3O_4	3

The soil had hardly drained after being constantly charged with electricity for 72 hours, so the experiment time was set to 72 hours. The measurement indices included the I, U, w, V, pH, S, and B. The initial w of the soil sample was measured before the experiments. Once the experiments were started, the V and I were recorded every hour, and the V and I were recorded every 2 hours after 24 hours. The U was measured every 12 hours. Once the experiment ended, the pH, S, and B of the soil samples were measured at varying distances from the anode. In addition, the w was determined and scanning electron microscopy (SEM) was performed on representative samples.

3. RESULTS AND DISCUSSION

3.1 Effect on I and U

The I during the EO process directly affects the energy consumed. Figure 2 shows the curve of I versus t in the presence of nano-SiO$_2$ and nano-Fe$_3$O$_4$. The I gradually decreased with t, which is inconsistent with the conclusion of Xie *et al.* [13]. This discrepancy was mainly caused by the difference in the salt content of the soil. When the salt content is low, the I has a downward trend; as salt increases, the I increases and then decreases.
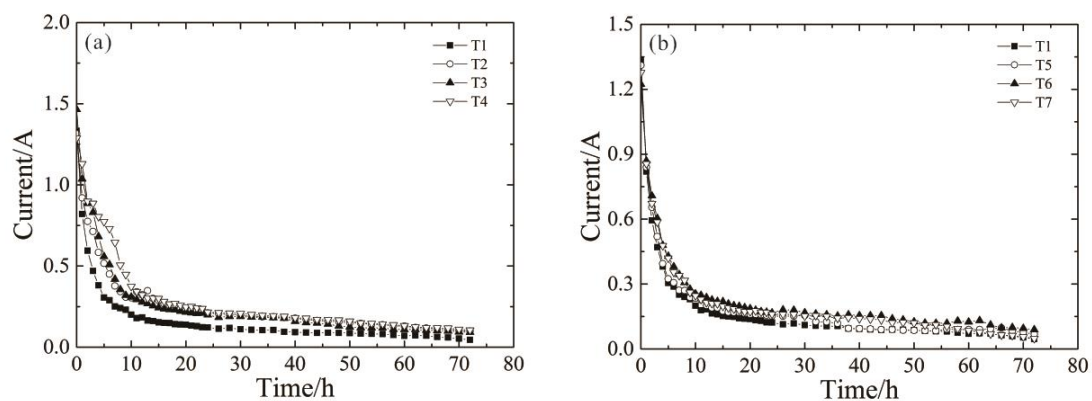
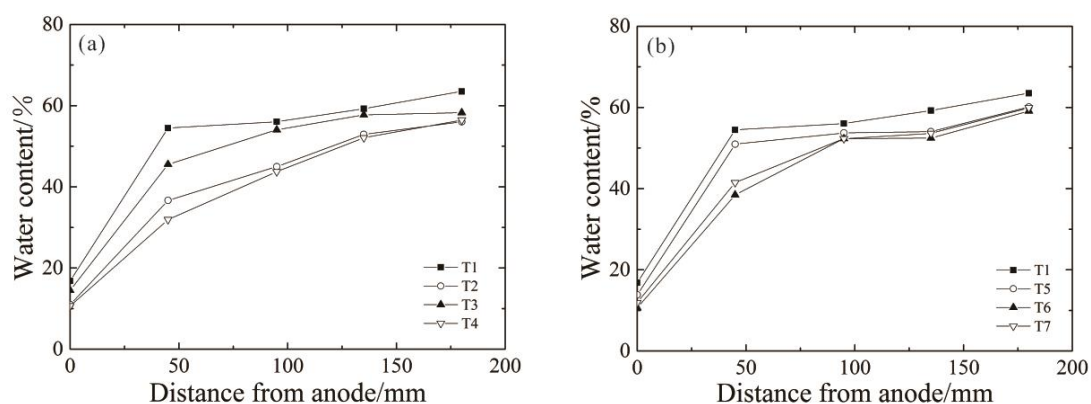**Figure 2.** Curves of I versus t (a) nano-SiO$_2$, (b) nano-Fe$_3$O$_4$
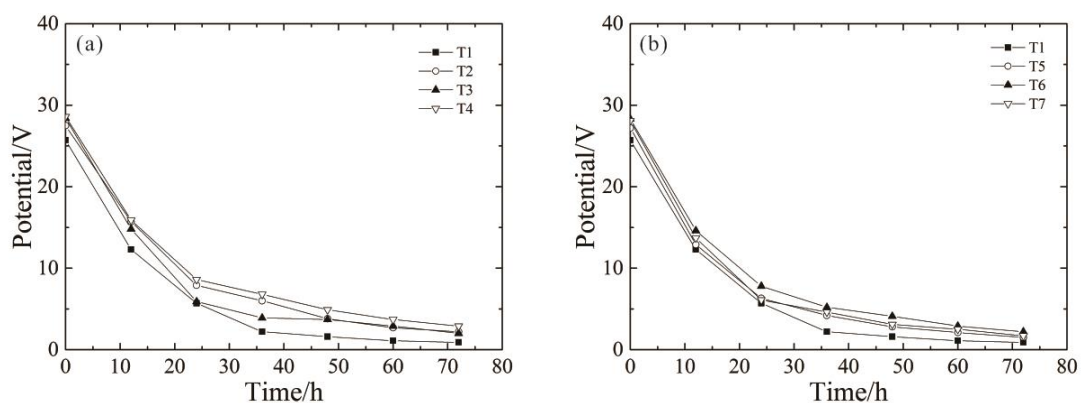
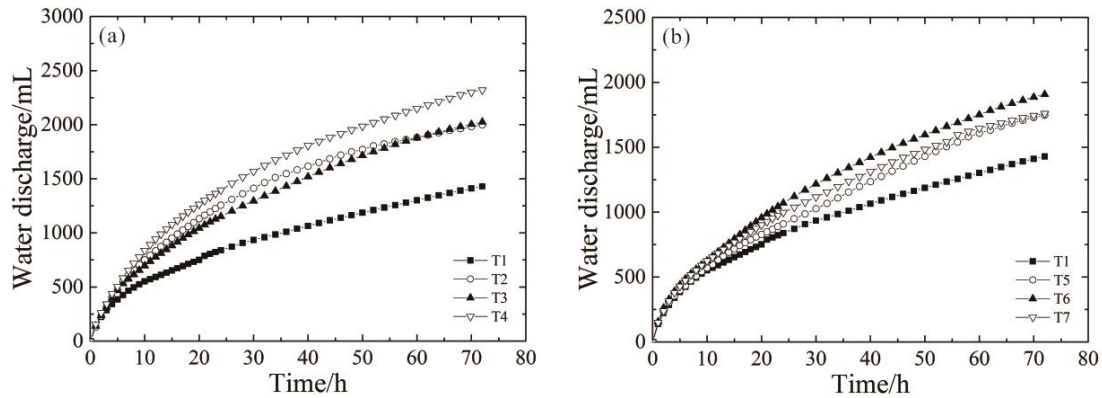**Figure 3.** Curves of U versus t (a) nano-SiO$_2$, (b) nano-Fe$_3$O$_4$

The silt soil used in this study had a low salt content, which caused a monotonic decrease in I over t [16]. In the initial stage (0-10 hours), the I declined rapidly and then slowly declined until it stabilized. The addition of nanomaterials slowed the decrease in I, and the influence became more obvious with an increase in concentration. With nano-SiO_2, T4 (3‰) and nano-Fe_3O_4, T6 (2‰) showed a relatively high I. Figure 3 shows the curve of U versus t in the presence of nano-SiO_2 and nano-Fe_3O_4. The U decreased with t, which is consistent with the conclusion of Jiao *et al*. [15]. The U decreased rapidly in the range of 0-36 hours and then gradually stabilized. Similar to the case of I, the highest U was achieved when the concentrations of nano-SiO_2 and nano-Fe_3O_4 were 3‰ and 2‰, respectively.

3.2 Effect on w and V

The V increased with t, while the w in the soil gradually decreased with t. Figure 4 shows the distribution of w versus anode distance. The w at the anode was relatively low and increased with the distance from the anode. In an electric field, cations in the soil migrate to the cathode and anions in the soil migrate to the anode. As the ions undergo directional movement, they drag the surrounding water molecules with them and form a directional seepage flow from the anode to the cathode [13]. The w in the soil was significantly reduced by the addition of nanomaterials, which indicates that the nanomaterials promoted EO drainage. Adding 2‰ nano-SiO_2 yielded the highest w in the area, followed by 1‰ and then 3‰. With nano-Fe_3O_4, the order was 1‰>3‰>2‰. Figure 5 shows the changes in V with t. The V increased with t, and the overall shape of the drainage curve was hyperbolic, which is consistent with previous studies [12, 17]. The addition of nanomaterials significantly increased the drainage of the soil, which indicates that nanomaterials promoted the EO drainage process and accelerated the soil consolidation. The drainage of the soil was maximized when the concentrations of nano-SiO_2 and nano-Fe_3O_4 were 3‰ and 2‰, respectively.
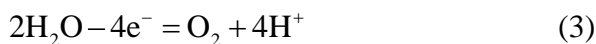

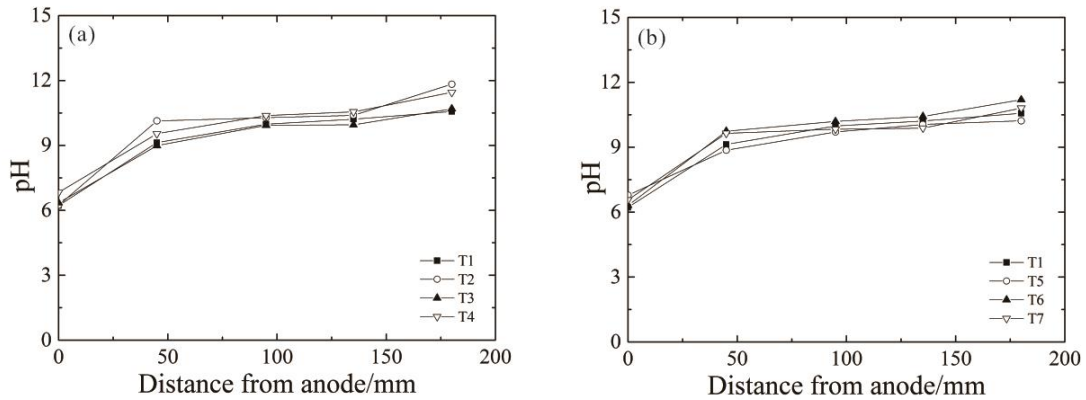**Figure 4.** Curves of w versus distance from anode (a) nano-SiO_2, (b) nano-Fe_3O_4

Figure 5. Curves of *V* versus *t* (a) nano-SiO_2, (b) nano-Fe_3O_4

3.3 Effect on pH

The change in pH is mainly caused by the different electric charges of the salts in the soil, and pH has a significant effect on the zeta potential. The absolute value of the zeta potential increases with pH and affects the electro-osmosis of the soil [18]. Figure 6 shows the distribution of pH versus the anode distance. The initial pH was 7.2 and nearly evenly distributed in the soil. After the EO treatment, the soil was almost alkaline, whereas the pH near the anode was low, which indicates that the soil was acidic near the anode. The pH increased with the distance from the anode, but the increase was not obvious. This finding is consistent with the results of Liu *et al*. [19]. The main reason for this phenomenon is that chemical reactions occurred at the anode (Equations (1-3)). A large amount of H^+ was produced and made the soil acidic. OH^- was generated at the cathode by reaction (Equation (4)) and made the soil alkaline [20]. In general, the pH was relatively low in the range 0-50 mm from the anode, and the pH remained unchanged in the range 50-200 mm from the anode. The distributions of pH were compared between the blank sample and the sample with the addition of nano-SiO_2 or nano-Fe_3O_4. The results concluded that the pH in the soil did not significantly change after the addition of nanomaterials.

$$Fe - 2e^- = Fe^{2+} \tag{1}$$

$$2Cl^- - 2e^- = Cl_2 \tag{2}$$

$$2H_2O - 4e^- = O_2 + 4H^+ \tag{3}$$

$$2H_2O + 2e^- = H_2 + 2OH^- \tag{4}$$

Figure 6. Curves of pH versus distance from anode (a) nano-SiO$_2$, (b) nano-Fe$_3$O$_4$

3.4 Effect on S and B

S is an important index of soil strength. Figure 7 shows the distribution of S versus anode distance. In general, the S of the soil near the anode was high and gradually decreased farther away, which was consistent with previous studies [15, 20]. The main reason for this phenomenon is that a directional seepage flow from anode to cathode formed under the electric field. At the anode, the w was low, and the S increased; at the cathode, the w was high, and the S decreased.
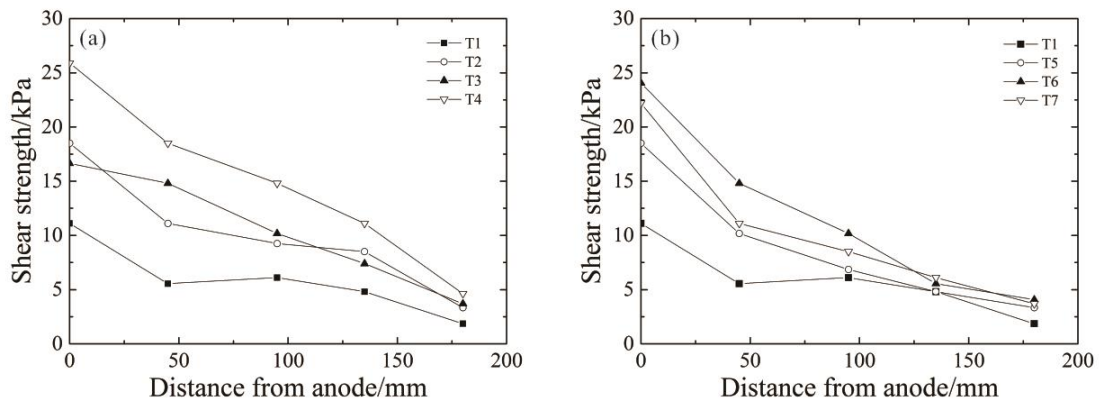
Figure 7. Curves of S versus distance from anode (a) nano-SiO$_2$, (b) nano-Fe$_3$O$_4$

The addition of nanomaterials greatly increased the S of the soil. With nano-SiO$_2$, the S was the highest when the concentration was 3‰; for nano-Fe$_3$O$_4$, the S was the highest when the concentration was 2‰. This finding is consistent with the w and V results. Figure 8 shows the distribution of B versus anode distance; the results are consistent with the conclusion of Sun *et al.* [21]. The B of the soil at the anode was significantly greater than that at the cathode, which was caused by the directional seepage flow. Similar to the case of S, the maximum B was achieved with 3‰ nano-SiO$_2$ and 2‰ nano-Fe$_3$O$_4$. The results analysis concluded that the addition of nanomaterials significantly improved the S and B of the soil, which indicates that nanomaterials promoted the EO consolidation of soil and there was a certain optimal concentration for each nanomaterial.
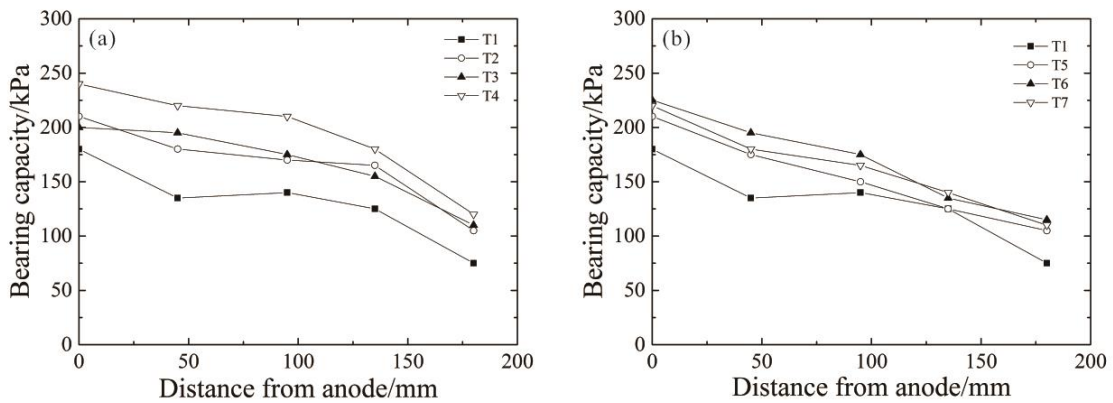
Figure 8. Curves of *B* versus distance from anode (a) nano-SiO₂, (b) nano-Fe₃O₄

3.5 Microscopic characteristics and crack distribution

In the EO drainage process, shrinkage occurred because of the decrease in soil *w*. The cracks distribution of soft soil addition with nano-SiO₂ is shown in Figure 9. The cracks were centered on the cathode and spread out in a cross pattern that extended to the anode, which is consistent with the study of Jiao *et al*. [15]. The main reason is that under the electric field, the water in the soil formed a directional seepage flow from the anode to the cathode. The *w* of the soil at the anode changed significantly, which caused serious shrinkage and crack formation.
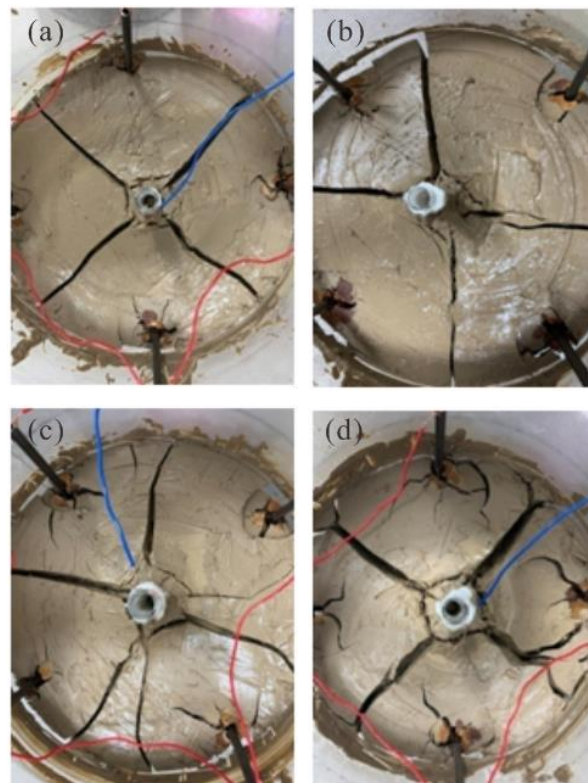
Figure 9. Curves of crack distribution (a) T1, (b) T2, (c) T3, (d) T4

The formation of cracks increases the energy consumption of EO, which increased electrode corrosion. During the experiment, a gray-green precipitate was observed on the anode electrode, because the metallic iron formed divalent iron ions in the EO process and these iron ions reacted with hydroxide ions to form Fe(II) hydroxide precipitates. Compared with the blank sample, the nano-SiO_2 sample had a significantly larger crack area. The higher is the nano-SiO_2 concentration, the greater is the crack area. At 3‰ nano-SiO_2, the crack area was the largest, the V was the highest, and therefore, the S and B reached the maximum values.

To accurately characterize the microstructure of the soil, SEM was performed on the samples that were collected at the anode after electro-osmosis (Figure 10). The soil after electro-osmosis exhibited a granular structure. Compared with the flocculation structure, the granular structure was denser and had a relatively small void ratio. Therefore, the interaction between the soil and the water was weakened, which was conducive to consolidation drainage.
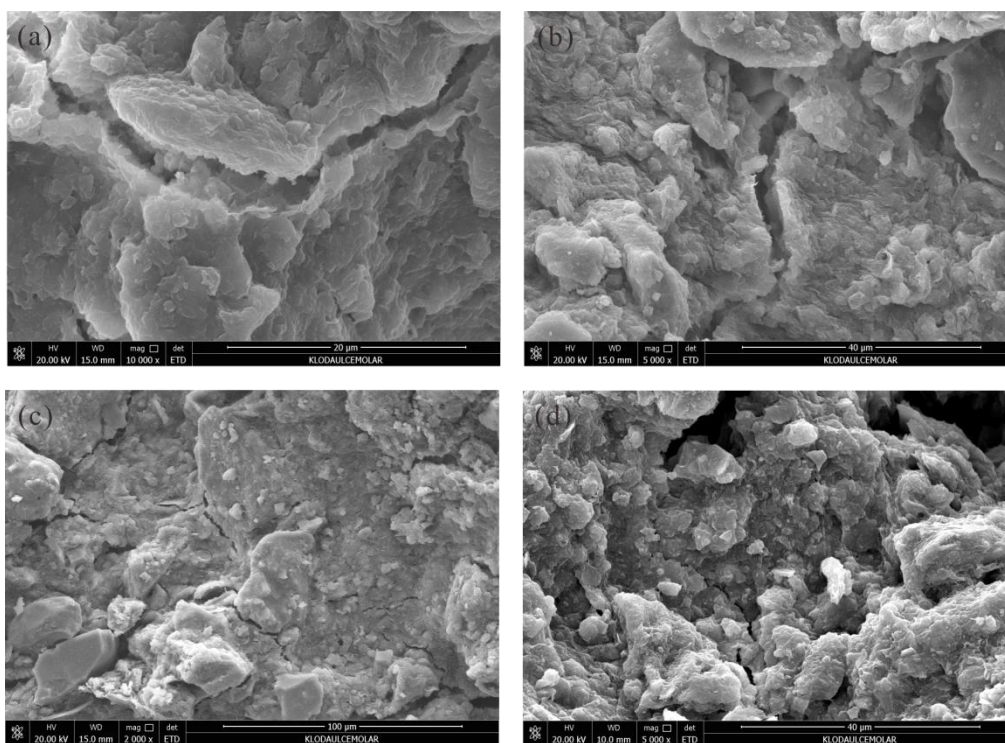
Figure 10. SEM image of soft soils (a) T1, (b) T2, (c) T3, (d) T4

In addition, during the electro-osmosis process, ion exchange occurred on the surface of the soil particles and inside the crystal layer. The metal ions released by the redox reaction at the anode entered the soil and exchanged with the ions on the surface of the soil particles and inside the crystal layer. Consequently, the electrical double layer became thinner, the zeta potential decreased, and the water absorption capacity of the particles was weakened [22-23]. As the thickness of the electric double layer decreased, part of the weakly bound water was released from the electrical double layer to form pore water and was then discharged under the electric field, which further reduced the w in the soil. As the drainage increased, the soil gradually consolidated, and the S and B also gradually

increased, which reflects the consolidating effect of EO. The size of the nanoaggregates that formed in the soil increased as the nano-SiO_2 concentration increased. However, SiO_2 nanoparticles had a minimal effect on filling the EO-produced cracks and could not effectively reduce the area of cracks. The 3‰ nano-SiO_2 sample showed the highest drainage, the largest crack area, and the largest nanoaggregates after EO, which indicates that a high concentration of nano-SiO_2 could better promote the EO. The better the drainage is, the lower the *w* is and the higher the *S* and *B* of the soil are.

4. CONCLUSIONS

EO consolidation of soft soil was carried out and promoted by the addition of SiO_2 nanoparticles or Fe_3O_4 nanosolution. During the experiment, the *I*, *U*, *w*, *V*, pH, *S*, *B*, crack distribution, and microstructure were measured. The following conclusions can be obtained:

(1) The effect of SiO_2 nanoparticles on the EO consolidation of soft soil was investigated. When the concentration of nano-SiO_2 was 3‰, the *V* was the highest, the *w* was the lowest, the *I* and *U* were the largest, the soil cracked the most, and the posttest *S* and *B* were the largest. The results indicate that the best concentration of nano-SiO_2 was 3‰, because it most promoted EO consolidation.

(2) The effect of Fe_3O_4 nanosolution on the EO consolidation of soft soil was investigated. The *I*, *U*, *w*, *V*, pH, *S*, *B*, and crack distribution were compared. The 2‰ nano-Fe_3O_4 solution most strongly promoted electro-osmosis, followed by 3‰ and 1‰.

(3) In the EO drainage process, the reduction in *w* caused soil shrinkage and crack formation. The crack area was centered on the cathode and spread out in a cross pattern that extended to the anode. When nano-SiO_2 was added, the crack area increased significantly. At the 3‰ nano-SiO_2 concentration, the crack area was the largest, the *V* was the highest, and the *S* and *B* were the highest.

(4) The granular structure of the soil caused a weakened interaction between the soil and the water, which promoted drainage consolidation. In addition, ion exchange occurred on the surface of the soil particles and inside the crystal layer, which produced a thinner electric double layer, lower zeta potential, and lower water absorption capacity of the particles. As the *V* increased, the soil gradually consolidated, and the *S* and *B* gradually increased, which reflects the mechanism of EO.

CONFLICT OF INTEREST
On behalf of all authors, the corresponding author states that there is no conflict of interest.

DATA AVAILABILITY
The data used to support the findings of this study are available from the corresponding author upon request.

References

1. A. L. Espinosa-Santiago and N. P. Lopez-Acosta. *Geotext. Geomembr.*, 48 (2020) 546.
2. G. Li, J. L. Zhang, Q. Yang and M. J. Jiang. *Eur. J. Environ. Civ. Eng.*, 21 (2017) 172.
3. Z. H. Sun, M. J. Gao and L. Xu. *Soil Mech. Found. Eng.*, 56 (2019) 59.
4. W. L. Zou, Y. F. Zhuang, X. Q. Wang, S. K. Vanapalli, Y. L. Huang and F. F. Liu. *Mar. Geores. Geotechnol.*, 36 (2018) 100.
5. L. M. Hu, L. Zhang and H. Wu. *J. Hazard. Mater.*, 368 (2019) 885.
6. L. Martin, V. Alizadeh and J. Meegoda. *Soils Found.*, 59 (2019) 407.
7. L. Martin and J. N. Meegoda. *Geotech. Test. J.*, 43 (2020) 791.
8. Z. J. Xue, X. W. Tang and Q. Yang. *Appl. Clay Sci.*, 141 (2017) 13.
9. F. Y. Liu, H. T. Fu, J. Wang, W. Mi, Y. Q. Cai and X. Y. Geng. *Soil Mech. Found. Eng.*, 54 (2017) 49.
10. H. Fu, Y. Cai, J. Wang and P. Wang. *Geosynth. Int.*, 24 (2017) 72.
11. F. C. Teng, S. C. Chien and C. Y. Ou. *J. Chin. Inst. Eng.*, 40 (2017) 25.
12. L. Zhang, N. W. Wang, L. P. Jing, C. Fang and R. Dong. *Rock Soil Mech.*, 40 (2019) 3493.
13. X. Y. Xie, Z. M. Li, L. W. Zheng, J. Z. Li and Y. M. Liu. *J. Cent. South Univ. (Sci. Technol.)*, 49 (2018) 655.
14. J. C. Zang, L. W. Zheng, X. Y. Xie, L. W. Cao and Z. M. Li. *J. Zhejiang Univ. (Eng. Sci.)*, 51 (2017) 245.
15. D. Jiao, X. N. Gong and Y. Li. *Chin. J. Rock Mech. Eng.*, 30 (2011) 3208.
16. Y. Li and X. N. Gong. *Chin. J. Geotech. Eng.*, 33 (2011) 1254.
17. F. Y. Liu, Z. Li, G. H. Yuan and J. Wang. *J. Civ. Environ. Eng.*, (2020). DOI: 10.11835/ j.issn. 2096-6717. 2020.064.
18. A. Kaya and Y. Yukselen. *Can. Geotech. J.*, 42 (2005) 1280.
19. F. Y. Liu, L. Zhang, J. Wang and B. Zhang. *J. Civ. Archit. Environ. Eng.*, 36 (2014) 52.
20. F. Y. Liu, Y. J. Wang and J. Wang. *China J. Highw. Transp.*, 29 (2016) 19.
21. Z. H. Sun, X. J. Yu, M. J. Gao and K. Wu. *Chin. J. Geotech. Eng.*, 39 (2017) 250.
22. J. Q. Shang, K. Y. Lo and R. M. Quigley. *Can. Geotech. J.*, 31 (1994) 624.
23. L. M. Vane and G. M. Zang. *J. Hazard. Mater.*, 55 (1997) 1.